The influence of Pt loading, support and nafion content on the performance of direct methanol fuel cells: examined on the example of the cathode

Xue, X.; Bock, C.; Birry, L.; MacDougall, B. R.

Publisher's version / Version de l'éditeur:
https://doi.org/10.1002/fuce.200900204
Fuel Cells, 11, 2, pp. 286-300, 2011-04-01

DOI: 10.1002/fuce.200900204

The Influence of Pt Loading, Support and Nafion Content on the Performance of Direct Methanol Fuel Cells: Examined on the Example of the Cathode

X. Xue[1], C. Bock[1]*, L. Birry[1], B. R. MacDougall[1]

[1] National Research Council of Canada, Institute for Chemical Process and Environmental Technology, 1200 Montreal Road, Ottawa, Ontario, Canada K1A 0R6

Received November 29, 2010 ; accepted December 14, 2010

Abstract

Nano-sized Pt colloids were prepared using the polyol method and supported on Ketjen black EC 600J (KB), Vulcan XC-72 (VC) and high surface area graphite 300 (HG). The effects of the Nafion ionomer content, and the Pt loading of the cathode catalyst layer as well as the Pt loading on the support on the performance of direct methanol fuel cells (DMFCs), were studied. The membrane electrode assemblies (MEAs) were analysed using current–voltage curves, cyclic voltammetry, electrochemical impedance spectroscopy (EIS) and adsorbed CO stripping voltammetry. Optimum Nafion to carbon (N/C) ratios (N/C being defined as the weight ratio of the Nafion ionomer to the carbon) were determined. The optimum N/C ratios were found to depend on the support as follows, 1.4, 0.7 and 0.5 for Pt/KB, Pt/VC and Pt/HG, respectively and to be independent of the Pt/C loading range of 20–80 wt% tested in this work. The highest DMFC performances, as well as the highest electrochemical active surface areas, and improved gas diffusivities, were achieved using these ratios. For the catalysts prepared in this work, the average Pt crystallite size was found to decrease with increasing surface area of the support for a particular Pt loading. MEAs made using KB as support and the optimal N/C ratio of 1.4 showed the best performances, i.e. higher than the VC and HG supports for any N/C ratio. The highest DMFC performance was observed using 60 wt% Pt on KB cathode electrodes of 1 mg Pt cm^{-2} loading and an N/C value of 1.4. For all three supports studied, the 60 wt% Pt on carbon loading resulted in the best DMFC performance. This may be linked to the Pt particle size and catalyst preparation method used in this work. In comparison to literature results, high DMFC performances were achieved using relatively 'low' Pt and Ru loadings. For example, a maximum power density of >100 mW cm^{-2} at 60 °C was observed using a 1 mg Pt cm^{-2} cathode loading and a 2 mg PtRu cm^{-2} anode loading.

Keywords: Cathode, DMFC, Nafion, Pt/Vulcan Catalyst, Supported Catalyst

1 Introduction

In recent years, proton exchange membranes fuel cells (PEMFCs) have attracted significant attention as alternative power sources due to their high energy density, low temperature operation and low pollution. The direct methanol fuel cell (DMFC) shows promising prospects as a potential source for micro- and portable electronic devices, as well as reduced emission power source for small vehicular applications [1–7]. Pt and Pt-based nanoparticles typically dispersed on high surface area carbon are used as electrocatalysts for both the anode and the cathode reaction. However, one of the significant obstacles for the commercialization of PEMFCs is the high cost of the membrane electrode assembly (MEA), which is in particular due to the high loadings of Pt-based catalysts needed to achieve reasonably high DMFC performances. It is

[*] *Corresponding author, christina.bock@cnrc-nrc.gc.ca*

well known that the Pt loadings can be reduced and the catalyst utilization can be increased by improving the activity of the electrocatalysts and by dispersing high surface area Pt catalysts, in the nano-size range, on the carbon supports [8]. The carbon support plays a vital role for the fuel cell performance. Vulcan XC-72, with the BET surface area of 250 m^2 g^{-1} and a mainly mesoporous structure, is the most commonly used catalyst support. High surface area carbon supports are important in order to obtain high catalyst surface areas per gram of carbon. The catalyst support material should have high electronic conductivity, high stability against corrosion, and preferably a mesoporous structure to allow for effective catalyst deposition, fuel access and water management [8]. Uchida [9,10] reported the effects of the microstructure of the catalyst layer on the performance of polymer electrolyte fuel cells (PEFCs) and reported that the pore-size distribution of the carbon support influences the performance of the fuel cell.

It is well known that properties of the catalyst layer such as catalyst loading, Nafion content, and the thickness of the catalyst layer affect the performance of a fuel cell (FC) [11–14]. Improvements in the FC performance can be achieved by increasing the electrochemically active surface area (EASA) of the catalyst layer. Furthermore, the FC reactions take place on the catalyst sites in contact with the Nafion. A Nafion membrane is typically used as electrolyte, however, the membrane does not soak deeply into the catalyst layer as a liquid electrolyte does. Thus, the reaction area is limited to the interface between the electrode and the membrane. As a result, the electrodes have low catalyst utilization and need high catalyst loadings [9,15]. Solutions of Nafion are impregnated into the electrode catalyst layer to increase the contact area between the Pt catalyst and the Nafion ionomer. In this way, the Pt utilization can be increased, resulting in higher FC performances if an optimum amount of ionomer is used [9–14].

The Nafion content in the electrode is generally expressed in mg cm^{-2}, i.e. the dry weight of Nafion ionomer divided by the geometric area of the electrode or as wt% of Nafion (dry weight of Nafion ionomer divided by the total weight of Pt + C and Nafion ionomer, multiplied by 100 [13]). The optimum Nafion content reported in the literature is generally in the range of 30–36 wt% irrespective of the Pt loading on Vulcan XC-72 for PEMFCs [11,16–18], while the optimal Nafion content seems to be ca. 22 wt% for DMFCs [19] Although many studies have reported the effect of the Nafion content, somewhat different optimum Nafion contents are reported by different researchers. Furthermore, it is to be expected that the optimum Nafion content required for high electrode and MEA performance depends on the microstructure of the support and possibly the Pt loading.

Song et al. [20] recently reported a novel preparation procedure for an electrocatalyst layer with high catalyst utilization for PEMFCs. It was found that the cathode prepared with a 46.3 wt% Pt, supported on high surface area carbon black, TEC 10E, Tanaka Kikinzoku Kogyo K.K ink at a Nafion to carbon (N/C) ratio of 0.7, exhibited a very high performance. For the efficient utilization of the Pt catalysts, the Nafion must be distributed uniformly and among the carbon and Pt catalyst without blocking access of the fuel to the catalyst sites. It has been recognised for some time that the optimal structure for high catalyst utilization is a catalyst layer that is thin, with an appropriate mixture of catalyst and ionomer [12,21].

In this work, a wide range of carbon supported Pt catalysts (Pt/C) are prepared. Three different support materials are used. In order to improve the utilization of the Pt catalyst particles, the effect of the Nafion content in the cathode layer is investigated as a function of Pt loading and support. DMFC performance curves are obtained. Cyclic voltammetry (CV), electrochemical impedance spectroscopy (EIS) and adsorbed CO (CO_{ads}) stripping measurements are conducted in full cell test stations to correlate electrochemical properties of the MEAs with the single cell DMFC performance.

2 Experimental

2.1 Preparation of the Carbon Supported Pt Catalysts

Details of the synthesis of the colloidal Pt catalyst solutions are described elsewhere [22,23]. The synthesis of the Pt colloids was carried out in ethylene glycol (Anachemia, ACS grade) containing sodium hydroxide (EM Science, ACS grade). First, 0.4652 g of $PtCl_4$ (Alfa Aesar, 99.9% metals basis) was dissolved in 50 mL of ethylene glycol containing 0.115 M NaOH. The solution was stirred for 30 min. in air at room temperature. Subsequently, the solution was heated and refluxed at 160 °C for 3 h, and then cooled in air. Dark brown solutions containing Pt colloids were formed in this manner. The colloidal solutions were mixed with appropriate amounts of the supports (i.e. Vulcan XC-72 (VC), Ketjen black (KB) EC-600J and Timrex HSAG300 (HG)) and are further referred to as Pt/C catalysts. The Pt loading on the support is given as wt% Pt. The wt% of Pt on a particular support is also given using the following type of abbreviation, e.g. VC-60 implying a 60 wt% Pt loading on Vulcan XC-72. It should be noted that for each Pt/C catalyst prepared in this work, clear filtrates were obtained after the dark brown colloidal solutions were mixed with the carbon supports for 12 h. This is taken as indication that the nominal and final wt% Pt/C values of the catalysts prepared in this work are the same. 0.5 mL of 0.5 M H_2SO_4 solution were added to the mixture to assist in the deposition of the Pt [22]. Furthermore, thermal gravimetric analyses (TGA) measurements were carried out in parrallel work that also suggest that the nominal and final wt% Pt/C values are the same.

2.2 Physical Characterization of the Supported Catalysts

A Scintag XDS2000 system was employed using a Cu Kα source to obtain XRD patterns of the supported Pt catalysts. The angle was extended from 20 to 75/ 2θ and was varied using a step size of 0.06°. Data were accumulated for 60 s per step. Silicon powder (typically 1–20 µm, 99.9985% purity,

Alfa Aesar) that was homogeneously grounded with the supported catalysts was used as an internal standard. XRD patterns of the Si-free and Si-containing samples were obtained for all the supported catalysts prepared in this work. A Philips CM 20 TEM was employed to measure the size of the 60 wt% Pt catalysts supported on Ketjen black. For the TEM analyses, the carbon supported catalyst powders were ultrasonically suspended in ethanol and a drop of the catalyst powder suspension was applied to a holey amorphous carbon film on 300 mesh Cu grid (Marivac, Limited).

2.3 Preparation of Electrodes and MEAs

The electrodes and membrane electrode assemblies (MEAs) were prepared as follows. The Pt/C catalysts prepared in this work were used as cathode catalysts, while a commercially available carbon supported catalyst consisting of 20 wt% Pt + 10 wt% Ru on Vulcan XC-72 (Alfa Aesar, HiSPEC 5000) was used as anode catalyst. Catalyst inks were prepared by dispersing appropriate amounts of the supported catalysts, distilled water, isopropyl alcohol (IPA) and Nafion® ionomer solution (Sigma–Aldrich, 5 wt% in lower aliphatic alcohols and water). The Nafion ionomer to the carbon support (N/C) ratios of the cathode were varied between 0.5 and 2.1, while the amount of ionomer in the anode was fixed at an N/C ratio of 0.7. In this work, the weight ratio of (N/C) is defined as the dry Nafion ionomer (W_{ion}) to the carbon support (W_{carbon}), while the Nafion content (wt% N) in the electrode is defined according to Eq. (1)

$$\text{Nafion content (wt.\%)} = \text{wt.\%N} = \frac{W_{ion}}{W_{catal} + W_{ion}} \times 100 \qquad (1)$$

In Eq. (1), W_{catal} is the weight of catalyst including the metal and the carbon support.

The anode and cathode catalyst inks were sprayed onto carbon paper (TGPH-060, E-Tek Co.) and formed into anode and cathode electrodes of noble metal weight of 2 and 1 mg cm^{-2}, respectively (unless otherwise stated). Subsequently, the anode and cathode electrodes were dried at room temperature. The Nafion contents of the electrodes prepared in this work are listed in Table 2.

The MEA was fabricated by hot-pressing the anode and cathode catalyst layers onto pretreated Nafion 117 membranes for 5 min. at 95 kg cm^{-2} at 135 °C. To fabricate the single DMFC, the MEA was sandwiched between two graphite current collectors with a serpentine design for the fuel and air distribution of 5 cm^2 geometrical active MEA area (Electrochem. Inc.). Current, power and impedance values are normalised for the 5 cm^2 geometrical area.

2.4 Single Fuel Cell Tests

The single cell consisted of two ribbed graphite plates, which were compressed between two gold plated stainless steel plates. These plates were provided with liquid and gas-feed tubes and were connected with the electric wires for the current/voltage measurements. Electrical heaters and a thermocouple were embedded into the plates to control the operating temperature of the FC. All experiments including electrochemical measurements were conducted in this cell.

2.4.1 Cyclic Voltammetry (CV)

CVs were recorded using an IM6 (Zahner, Germany) potentiostat and frequency analyser. For CV studies, humidified nitrogen at 100 sccm was fed to the cathode about 10 min to remove the oxygen, then 2 sccm of distilled water was fed to the cathode, which served as the working electrode. Humidified hydrogen (8% H_2 in Argon) was fed to the anode at 200 sccm. The latter served as counter electrode and dynamic hydrogen reference electrode (DHE). The potential was scanned at 50 mV s^{-1} between 0 and 1.2 V *versus* the DHE. All potentials are referred *versus* the DHE in this work. For all CV studies, the cell temperature was maintained at 40 °C.

2.4.2 Adsorbed CO (CO_{ads}) Stripping Measurements

CO_{ads} stripping measurements were carried out using a Solartron 1287 potentiostat/galvanostat interfaced with a GPIB card to a personal computer. The oxidation of CO_{ads} was used to determine the electrochemical active surface area (EASA) of the Pt catalyst in the cathode. For the CO_{ads} stripping measurements, humidified hydrogen (8% H_2 in Argon) was fed to the anode and humidified CO (99.99% pure gas) was fed to the cathode for 20 min. to allow for complete adsorption of CO onto the Pt catalyst sites, while the cathode (in this case the working electrode) was kept at 0.1 V. Excess CO was then purged from the cathode layer with N_2 for 70 min, while the potential was maintained at 0.1 V. Two CV cycles were recorded at 10 mV s^{-1} between 0 and 1.2 V. The first sweep was performed to electro-oxidise the CO_{ads}, while the second cycle was used as background and to verify that excess CO_{ads} was indeed removed from the catalyst layer. The EASA of the Pt catalyst was estimated from the CO_{ads} stripping charge (Q_{COads}) assuming a monolayer of linearly adsorbed CO, i.e. a charge to EASA conversion factor of 420 μC cm^{-2} was used [24,25]. The CO_{ads} stripping measurements were repeated after three days of cell operation.

2.4.3 Current–Voltage Curves

A peristaltic pump (Ismatec IPC 4, Cole-Parmer Inst. Co.) was employed to supply aqueous 1 M methanol solutions to the anode at 2 mL min^{-1}. Oxygen was fed to cathode at 100 sccm and at atmospheric pressure. The cell temperature was varied between 40 to 70 °C. Oxygen gas was humidified by passing through a humidifier (Electrochem. Inc.) at 40 °C. Current–voltage curves were measured galvanostatically using an electronic load (Keithley 2440, Alliance Test Equipment, Inc.). Prior to the measurements, the cell was operated at 0.4 V and 40 °C for 2 h to condition the MEA. We have

found that the cell performances stabilised within three days of measurements. All current–voltage polarization curves presented here were measured after 3-days of repeated conditioning and measuring the cell performance.

2.4.4 Electrochemical Impedance Spectroscopy (EIS)

EIS was carried out using an IM6 (Zahner, Germany) potentiostat and frequency analyser. The cells were maintained at 40 °C between the frequency range of 50 kHz to 50 mHz. Impedances were measured under galvanostatic control of the cell. The amplitude of the sinusoidal current signal did not exceed 10 mA. In order to separate the recorded impedances of the anode and cathode, the anode impedance was measured separately by supplying humidified hydrogen (8% H_2 in Argon) and aqueous 1 M methanol solutions to the cathode and anode sides, respectively. In this method, the cathode acts as a DHE. Proton reduction at the cathode is much faster than methanol oxidation at the anode, hence, the impedance contribution of the cathode can be neglected [26–28]. The anode impedance is subtracted from the total cell impedance measured under oxygen/1 M methanol solution feed, resulting in the cathode impedance spectrum.

3 Results and Discussion

3.1 Effect of the N/C Ratio for Different Carbon Supports on the DMFC Performance

Catalysts of various Pt loadings between 20–80 wt% on three different supports were prepared in this work. Properties reported in the literature for the three different supports are summarised in Table 1. Figure 1 shows typical X-ray diffraction (XRD) patterns obtained for supported Pt catalysts prepared in this work. XRD patterns for the example of 60 wt% Pt/C catalyst loadings on the different supports are shown. Scherrer's formula [29,30] was used to calculate the average Pt crystallite size (d_{Pt}) from the Pt (220) peak, which is also listed in Table 1. For CV studies, humidified nitrogen at 100 sccm was fed to the cathode about 10 min to remove the oxygen, then 2 sccm of distilled water was fed to the cathode as a working electrode. which served as the working electrode. The most promising Pt/C catalysts studied in this work, i.e. the 60 wt% Pt catalyst supported on Ketjen black was also investigated by TEM. A typical TEM image and corresponding histogram is shown in Figure 2. The TEM analysis suggests the average particle size of the KB-60 catalysts to be 2 ± 1 nm. This is in good agreement with the results estimated from the XRD data. Furthermore, the TEM image shown in Figure 2 (a) reveals that catalyst agglomeration of this as-prepared catalyst is minimal.

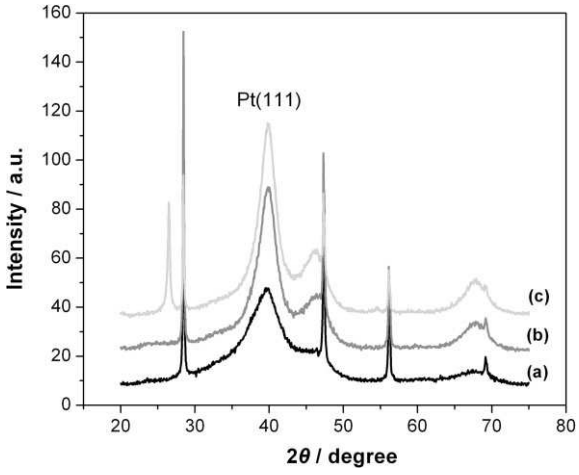

Fig. 1 Slow scan XRD patterns for supported Pt catalysts of 60 wt % catalyst loading. Si powder was added to the catalysts as internal standard. (a) Ketjen black support (EC-600J), (b)Vulcan XC-72 and (c) Timcal high surface graphite support.

3.1.1 Optimum N/C Ratio

A goal of this work is to find the optimal Nafion content in the electrode layer for different carbon supported Pt catalysts. It is well known that the N/C ratio is a crucial factor for the performance and stability of a FC [11,12]. The DMFC performances, i.e. current–voltage and the resulting power curves, for MEAs consisting of cathodes made of different N/C ratios are shown in Figure 3. Figure 3 (a)–(c) show the result for the

Table 1 Technical data[a] of the three supports used in this work and some charateristics for 60 wt% Pt/C loading catalysts.

Company name	Carbon support name	Type	Average support particle size / nm	Support surface area/ m^2/g	Support pore volume (DBF) / mL/g	Support apparent bulk density / g cm^{-3}	dPt[b] / nm	Sample abbreviation for 60 wt% Pt/C loadings
Ketjen black int.[c]	EC 600 J	Furnace black	~30	~1300	~0.31–0.345	0.125–0.145	2.2	KB-60
Cabot corp.[d]	Vulcan XC-72	Furnace black	~50	~250	~0.32	0.264	3.5	VC-60
Timcal Graphite & Carbon.[e]	HSAG-300	Graphite	15 (min) crystallite Height	250 (min) 280	n.a.	0.3	3.7	HG-60

[a]Technical data of the supports from product data sheet published on the web.
[b]Average Pt crystallite size (d_{Pt}) estimated from the corresponding XRD pattern using the highest intensity, the Pt(220) peak and Scherrer's equation. It should be noted that d_{Pt} was found to depend on the Pt/C loading, as discussed later in this work.
[c] http://www.akzonobel-polymerchemicals.com/.
[d] http://www.cabot-corp.com/.
[e] http://www.timcal.com/.

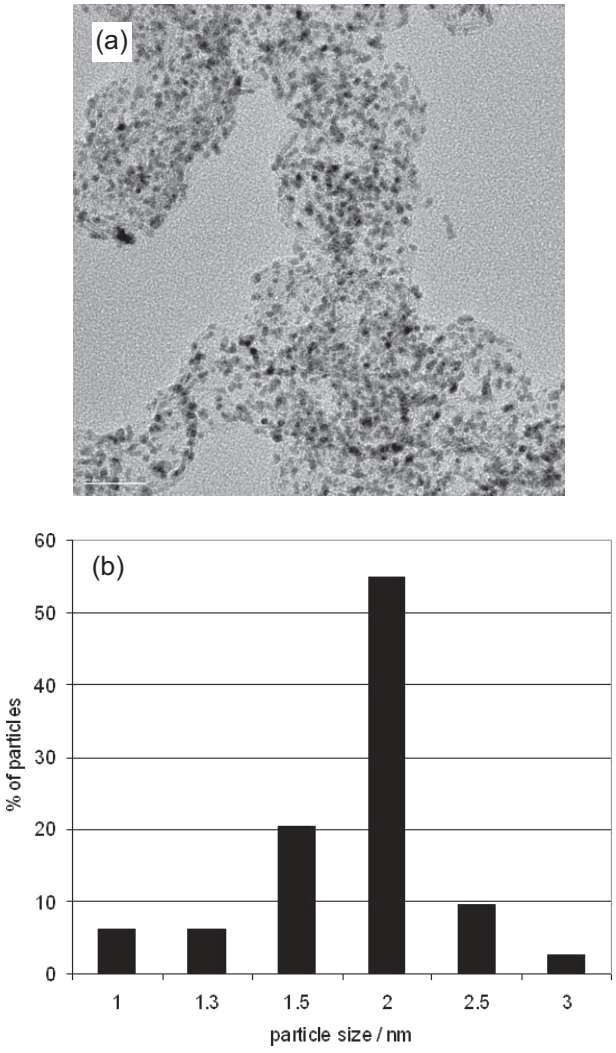

Fig. 2 (a) TEM images and (b) corresponding histogram of 60 wt% Pt catalyst deposited on Ketjen black (EC-600J) support. The image is obtained at a magnification of 135 kx and the bar in Figure 2 (a) indicates a scale of 20 nm.

three different supports. The same Pt loading was used for all three supports, namely 60 wt% Pt/C, as this Pt/C loading was found to result in the best DMFC performance. For the KB-60 cathode catalyst (shown in Figure 3 (a)), the performance is seen to increase with increasing N/C ratio from 0.7 to 1.4, while a further increase in the N/C ratio from 1.8 to 2.1 results in a decrease in the DMFC performance. In case of the KB support, the cathode made using an N/C ratio of 0.7 gives a very poor performance, while a much better performance is achieved using an N/C ratio of 1.4. Additional experiments, not shown here, were conducted using MEAs made of cathodes consisting of 20, 40 and 80 wt% Pt loadings on KB for the entire range of N/C ratios, i.e. from 0.5 to 2.1. The results showed that for all Pt/C loadings on KB, the N/C ratio of 1.4 exhibited the highest DMFC performance. The reproducibility of the measurements was tested by measuring the performance curves for three MEAs prepared in the same manner. The peak power density values were measured to be within ± 5%.

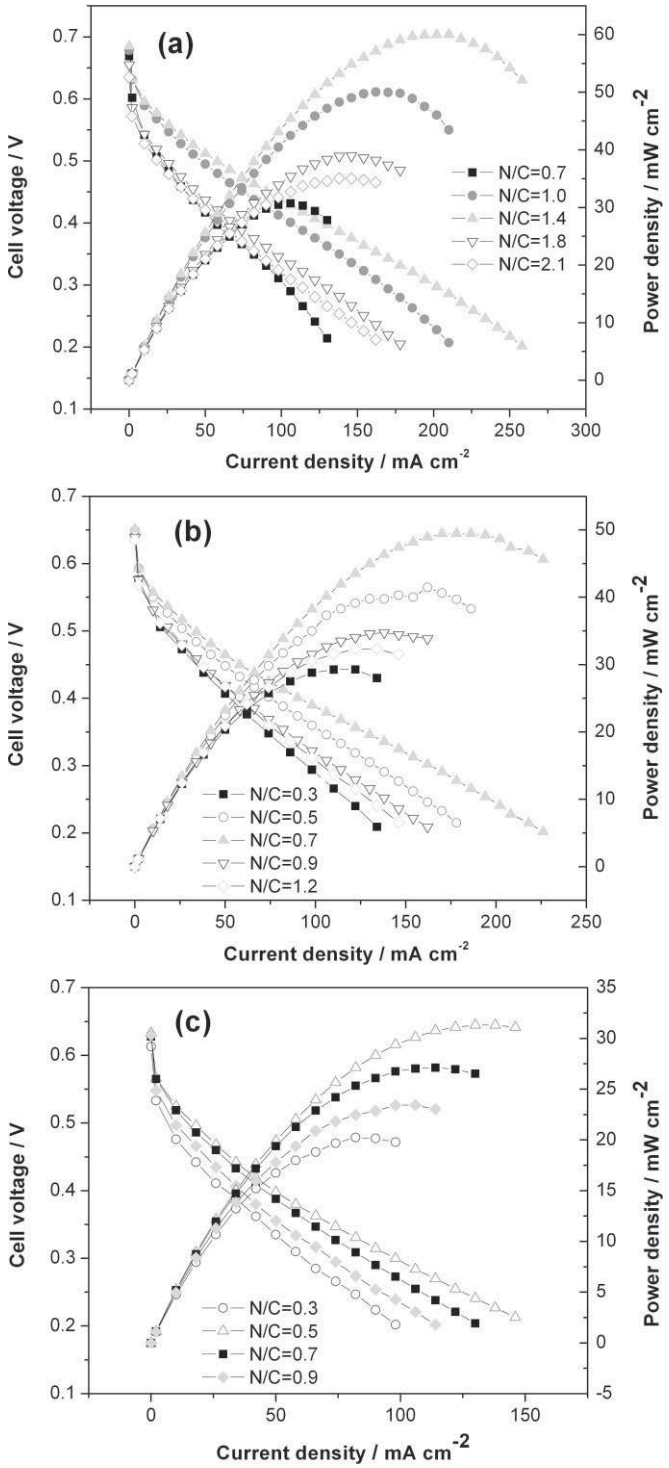

Fig. 3 DMFC performances as a function of the ionomer content and the catalyst support of the cathode layer. (a) shows the result for the KB-60 cathode catalyst, (b) for the VC-60 and (c) for the HG300-60 cathode catalysts.

Effects of the N/C ratio on the DMFC performance for the other 60 wt% Pt cathode catalysts supported on VC and HG are shown in Figure 3 (b) and (c). Similar to the case of the KB support, the DMFC performances using VC and HG cathode catalyst layers show a maximum for a specific N/C ratio.

However, the optimum N/C ratios are found to be lower, namely 0.7 and 0.5 for the VC and HG supports, respectively. The optimum N/C value using VC as catalyst support is essentially the same as reported by Liu and Song et al. [19,20] i.e. ~22 wt%, thus supporting the results obtained in this work. It is known that a higher Nafion content in the catalyst layer enhances the proton conductivity [31,32], while it increasingly blocks the access of the O_2 fuel to the catalyst sites. In fact, the sites active for the O_2 reduction in the catalyst layer are made of a triple interface that consists of the catalyst site on the electron conductor, the proton conductor and the gaseous O_2 reactant. High local O_2 reduction currents are achieved for the catalyst sites that are simultansouly connected to electronic as well as protonic conductive phases, in combination with a high local (at the catalyst site) O_2 concentration. The optimum N/C ratio of a catalyst layer reflects the balance between optimised proton conductivity and fuel access within the entire layer [11,12]. Both of these factors, i.e. the proton conductivity and the access of the O_2 fuel depend on the distribution of the Nafion within the porous and three dimensional network of the catalyst layer. The surface area, particle size, surface functional group, and porosity of the three supports used in this work are different (see, e.g. Table 1). Therefore, it is to expect that the optimal N/C ratio, which is influenced by the Nafion distribution within the catalyst layer, depends on the support. In fact, the optimal N/C ratios determined in this work suggest that the highest amount of Nafion is needed to reach the optimal proton conductivity and fuel access balance for the KB support. The surface area of the KB support is substantially larger than for the VC and HG supports (Table 1). Therefore, it is to expect that a higher amount of Nafion (higher N/C ratio) is needed to achieve a continous network of Nafion within the catalyst layer that allows for an effective conduction of protons within the layer, and also, connects the catalyst sites, thus maximising their utilization. The N/C ratios, for the VC and HG supports are relatively similar, which appears consitent with the essentially same surface area of the two supports. The slight difference in the optimal N/C ratio for the VC *versus* the HG support is likely due to other differences of these support such as particle size, shape and microporosity. The hydrophobic properties of the three carbon supports are also different, for example the HG support itself is more hydrophilic than the VC and the KB support. It is known that the hydrophicity of the electrode layer influences the water management and O_2 access to the catalyst sites. Neverthless, the

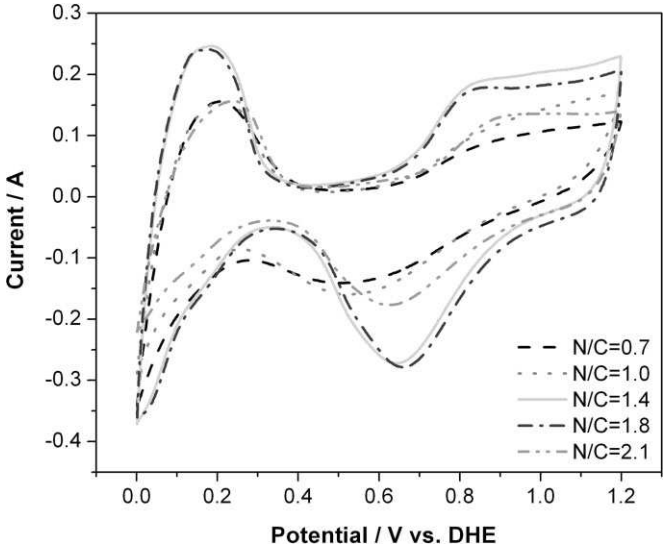

Fig. 4 Cyclic voltammograms for various N/C ratios of the cathode layer. The example of the KB-60 cathode catalyst is used. The CVs are recorded at 50 mV s^{-1} in the DMFC at a cell temperature of 40 °C.

Table 2 Electrode parameters for different N/C ratios of the cathode catalyst layer[a].

Cathode catalyst	Sample number	Pt surface area[b] / $m^2 g^{-1}$ Pt	N/C ratio[c]	Cathode ionomer content wt% N[d]	d_{MEA} / µm	OCP / V	EASA[e] / $m^2 g^{-1}$ Pt	Pt utilization[f] /%
KB-60	1	127.4	0.7	21.9	547	0.67	61.9	48.6
	2		1.0	28.6	543	0.68	70.6	55.4
	3		1.4	35.9	546	0.68	78.3	61.5
	4		1.8	41.9	544	0.66	70.9	55.7
	5		2.1	45.7	554	0.64	63.3	49.7
VC-60	1	80.1	0.3	10.7	526	0.64	37.8	47.2
	2		0.5	16.7	529	0.65	48.5	60.5
	3		0.7	21.9	534	0.65	60.7	75.8
	4		0.9	26.5	545	0.64	40.3	50.3
	5		1.2	32.4	549	0.63	38.4	47.9
HG-60	1	75.8	0.3	10.7	533	0.61	33.8	44.6
	2		0.5	16.7	537	0.63	50.0	66.0
	3		0.7	21.9	537	0.63	43.4	57.3
	4		0.9	26.5	543	0.63	37.2	49.1

[a] In all cases, 60 wt% Pt/C and 1 mg Pt cm^{-2} membrane area loadings are used.
[b] Pt catalyst surfaces areas estimated using XRD data and Eq. (2). The values obtained in this manner represent a rough estimate, as discussed in the text.
[c] Weight ratio of Nafion in the cathode layer to carbon black, as defined on p. 3.
[d] Nafion content in wt% of the cathode. The values are calculated using Eq. (1).
[e] Pt surface area measured from CO_{ads} stripping voltamograms.
[f] % Pt utilization, which is the ratio of the Pt surface area estimated from CO_{ads} stripping experiments (column 7) and divided by the theoretical Pt area (column 2).

DMFC performance of the electrode layer made with the HG support is not higher than observed for less hydrophobic supports. This likely reflects the fact that the electrochemically active catalyst surface areas are different, and possibly also that the overall electrode properties and other hydrophobic properties of the electrode layer (induced by e.g. a balance provided by possibly an optimum N/C ratio) affect the resulting performance.

In summary, the results suggest that the nature of the carbon support, rather than the Pt loading per membrane area, determines the N/C ratio, at least for the Pt/C loading in the range of 20–80 wt% Pt/C studied in this work. It is possible that the optimum N/C ratio is different from the presently reported values for very high metal catalyst loadings, when the catalyst itself may become the effective support.

3.1.2 *More Detailed Studies of the Impact of the N/C Ratio*

Additional electrochemical analyses of the MEAs were carried out to further study the effect of the different N/C ratios. CVs were recorded to probe the protonic and electronic access to the Pt nanoparticles within the cathode catalyst layer. Figure 4 shows typical CVs for MEAs made of cathodes using the KB-60 catalysts and different N/C ratios. It is seen that the hydrogen adsorption/desorption charge (Q_{Hads}/Q_{Hdes}) is the highest for the N/C ratios of 1.4 and 1.8. This suggests a higher EASA of the Pt catalysts. This increase results from an increase in interfacial area between the Pt catalyst particles and the Nafion. This, in turn, also increases the number of active catalyst sites available for the oxygen reduction reaction (ORR).

In addition, the Pt EASA of the cathode catalyst layer was estimated using CO_{ads} stripping measurements. Figure 5 shows the CO_{ads} stripping voltammograms of the cathode catalyst layers. The values are listed in Table 2. The EASA values extracted from CO_{ads} stripping voltammetry show the same trend as the H_{ads}/H_{des} charge (within the experimental error of 10%), and show a maximum for the optimum N/C ratios of a particular carbon support. To estimate the Pt/C catalyst utilization, the EASA values are divided by the theoretical Pt surface area, and multiplied by 100. Assuming spherical Pt particles and no agglomeration, a rough estimate of the theoretical surface area is obtained using the following equation [29].

$$S_T = \frac{6000}{\rho \times d} \tag{2}$$

In Eq. (2), d is the average particle sizes in nm, S_T the theoretical surface area in $m^2\ g^{-1}$ and ρ the density of Pt, namely 21.4 g cm^{-3}. The calculated results are summarised in Table 2. They suggest that an increase the N/C ratio increases the utilization of Pt, e.g. in case of the KB support, an increase in the N/C ratio from 0.7 to 1.4 increases the Pt utilization by ca. 13% from 48.6 to 61.5%. This is likely due to an increased interfacial area between the electrolyte membrane and the catalyst layer, i.e. reflecting an improved protonic connection within the catalyst layer achieved by the higher Nafion content. However, the Pt utilization decreases to 49.7% upon increasing the N/C ratio to 2.1. Consistent with literature views [11,12], this decrease likely reflects the blockage of catalyst particles by excessive amounts of the Nafion ionomer. These particles are, therefore, not accessibly for the O_2 reactant.

Figure 6 (a) and (b) show the EIS results presented in the form of Nyquist plots for the total cell and the anode impedance, respectively. The EIS spectra were recorded using the KB-60 cathode catalyst, a cell temperature of 40 °C and a current density of 100 mA cm^{-2}. The results for different N/C ratios are shown. The total impedance curves, Figure 6 (a), are found to be made of two overlapping semi-circular loops. The two loops are assigned to the anode and cathode reaction, i.e. the methanol oxidation reaction (MOR) and the oxygen reduction (ORR), respectively. The characteristics of the anode layer are seen in the loop at lower frequencies, while the loop at higher frequencies reflects the cathode layer. This is a simplified approach adopted for the purpose of this study, which intends to demonstrate changes in the cathode layer in a semi-quantitative rather than detailed manner. The high frequency intercept and the diameter of the semicircle are assigned to the internal ohmic resistance of the total fuel cell ($R_{\Sigma\Omega}$) and to the charge transfer resistances of the cathode and anode ($R_{\Sigma CT}$), respectively. $R_{\Sigma\Omega}$ represents the sum of the uncompensated resistances for the anode ($R_{A\Omega}$) and cathode

Table 3 Resistance data extracted from EIS results for different N/C ratios of the cathode made using the KB-60 catalyst[a].

N/C[b]	Wt% N[c] /%	$R_{\Sigma\Omega}$[d] / Ω cm^2	$R_{\Sigma CT}$[d] / Ω cm^2	$R_{A\Omega}$[d] / Ω cm^2	R_{ACT}[d] / Ω cm^2	$R_{C\Omega}$[d] / Ω cm^2	R_{CCT}[d] / Ω cm^2
0.7	21.9	0.565	1.57	0.36	1.18	0.205	0.39
1.0	28.6	0.51	1.45	0.43	1.075	0.08	0.375
1.4	35.9	0.37	1.405	0.365	1.105	0.005	0.3
1.8	41.9	0.37	1.815	0.355	1.175	0.015	0.64
2.1	45.7	0.515	1.71	0.38	1.14	0.135	0.57

[a] In all cases 1 mg Pt cm^{-2} and 2 mg Pt-Ru per cm^{-2} loadings at the cathode and anode, respectively are used.
[b] Weight ratio of Nafion in the cathode layer to carbon black, as defined on p. 3.
[c] Nafion content in wt% of the cathode. The values are calculated using Eq. (1);
[d] Resistance values, as defined in detail in the text. Section 3.1.2 $R_{\Sigma\Omega}$ and $R_{\Sigma CT}$ stand for the total uncompensated cell and total cell charge transfer resistance, respectively. $R_{A\Omega}$ and R_{ACT} stand for the uncompensated anode and the anode charge transfer (MOR) resistance, respectively. Similarly, $R_{C\Omega}$ and R_{CCT} stand for the uncompensated cathode and the cathode charge transfer (ORR) resistance, respectively. The total cell and anode resistance values are measured (Figure 6 (a) and (b), respectively), while the values for the cathode resistances are calculated by subtracting the anode impedances from the corresponding total cell impedances.

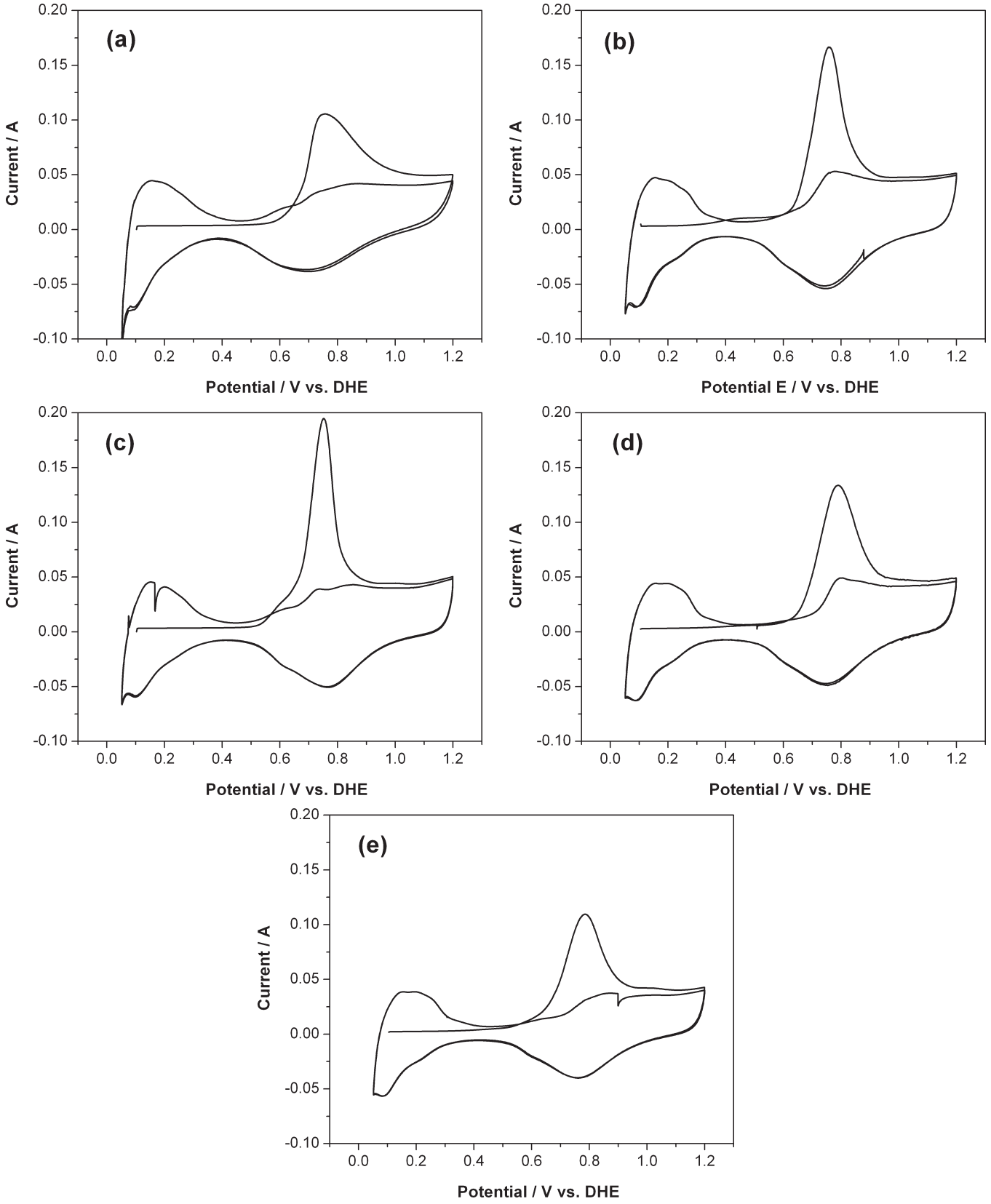

Fig. 5 CO_{ads} stripping voltammograms for various N/C ratios of the cathode layer. (a) N/C = 0.7, (b) N/C = 1.0, (c) N/C = 1.4, (d) N/C = 1.8, (e) N/C = 2.1. The example of the KB-60 cathode catalyst is used. The stripping CVs are recorded at 10 mV s^{-1} in a DMFC using a cell temperature of 40 °C.

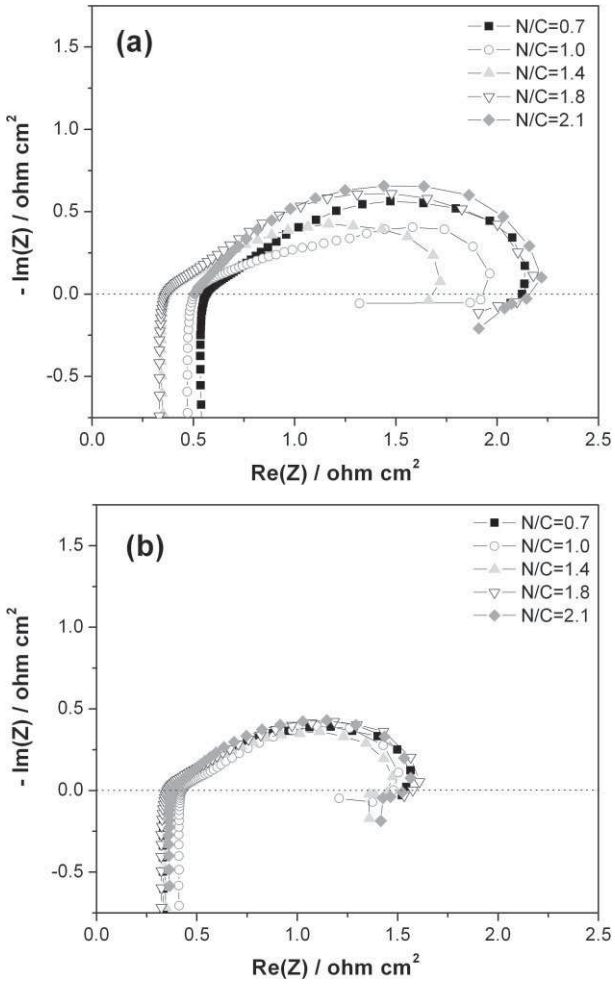

Fig. 6 Electrochemical impedance spectra as a function of the N/C ratio of the cathode layer. In all cases, the KB-60 cathode catalyst is used. The spectra are recorded for a DMFC working mode at 100 mA cm^{-2} and at a cell temperature of 40 °C. (a) shows the total cell impedance. An aqueous 1 M methanol solution is fed to the anode at 2 mL min^{-1}, while the cathode is supplied with O_2 at 100 sccm. (b) shows the anode impedance recorded using the same conditions as for Figure 6 (a), except that the cathode is used as DHE, as described in the experimental section.

($R_{C\Omega}$) catalyst layers, the membrane, the carbon paper, the graphite end plates and the contact resistance between them. $R_{\Sigma CT}$ represents the charge transfer resistance of the MOR (R_{ACT}) and the charge-transfer resistance of the ORR (R_{CCT}). It should be noted that the cathode spectra is calculated by subtracting the measured anode spectra from measured spectra of the full cell. Hence, the $R_{A\Omega}$ value measured at high frequencies also contains the resistance of the membrane, while the calculated $R_{C\Omega}$ value is small, consistent with results reported in the literature [14,,28,33,34]. The values of all resistance parameters derived from the EIS results shown in Figure 6 (a) and (b) are listed in Table 3. The Nyquist plots for the anode, Figure 6 (b), are seen to be essentially the same for all MEAs. This is to be expected as the anode composition is the same in all MEAs studied in this work. This result also suggests that the MEAs are made in a reproducible manner. The anode impedance is subtracted from the total cell impedance, resulting in the values for the cathode impedance, which are listed in Table 3. The $R_{C\Omega}$ and R_{CCT} value is the smallest for the N/C ratio of 1.4. The smaller number results from the fact that the increased N/C ratio enhances the proton conductivity of the catalyst layer and connects catalyst sites. However, the Nafion also acts as an electric resistance, as well as a resistance to oxygen diffusion, thus being responsible for the observed increase in the R values with larger N/C ratios. The EIS results are consistent with the DMFC performance curves, as they again suggest an optimal N/C ratio of 1.4 for cathodes made using the Pt supported on KB. Similar results were obtained for MEAs made using the VC-60 and HG-60 cathode catalysts. For these supports, the EIS results suggest optimum N/C ratios of 0.7 for the VC and 0.5 for the HG support.

3.2 Effect of the Carbon Support on the DMFC Performance

Ketjen black (EC600J), Vulcan XC-72 and high surface area graphite (HSAG 300) are used as supports for the cathode catalysts in this work. Table 1 summarises properties for 60 wt% Pt/C loadings for all three supports. The surface areas of the three carbons are also listed in Table 1. The same preparation method is used for the three supports, i.e. identical Pt colloidal solutions are deposited onto the three supports. Nevertheless, the Pt particle size is seen to depend on the support material. The Ketjen black (EC600J) has the highest surface area of about 1300 m^2 g^{-1}, while the surface areas of Vulcan XC-72 and HSAG 300 are very similar, namely 250 m^2 g^{-1}. For the catalysts prepared in this work, the average Pt particle size for the 60 wt% Pt/C loadings is the smallest, 2.2 nm for the highest surface area support, KB and 3.5 and 3.7 nm for the VC and HG supports, respectively. Due to the small particle size of the Pt, the EASA is expected to be larger for the 60 wt% Pt/C catalysts than the other Pt/C loadings. It is well known that uniform distribution of the catalyst particles and an optimum, 'small' catalyst particle size are important factors for the stable and efficient operation of FCs [3–5]. For the ORR, an optimal Pt particle size of ca. 3.5 to 4 nm has been suggested [35–37]. However, the results of this work suggests that the best performance is achieved for the KB-60 catalyst consisting of 2.2 nm average size Pt particles. It is unclear if the better performance is related to the particle size and/or the different properties of the carbon support. It should also be noted that the particle sizes listed in Table 1 are average numbers estimated from XRD patterns of the as-prepared catalysts and the actual particle size in the operating cathode of the FC may be different.

Figure 7 shows DMFC performances at 40 °C using KB-60, VC-60 and HG-60 cathode catalysts and an N/C ratio of 0.7 for all cathode layers. MEAs consisting of cathodes made using the VC-60 catalyst show a better performance than the KB-60 and HG-60 catalysts. However, from the experimental results of Section 3.1, it was found that the optimum N/C value for KB, VC and HG are 1.4, 0.7 and 0.5, respectively. There-

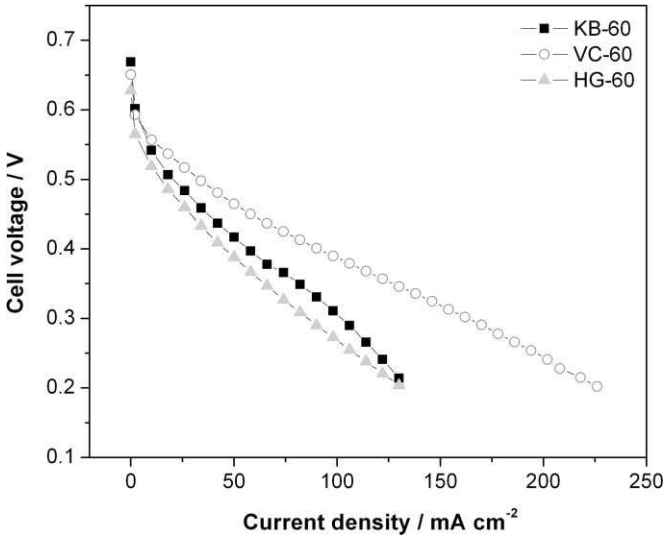

Fig. 7 DMFC performances shown as cell voltage *vs.* current density plot for KB-60, VC-60 and HG-60 cathode catalysts, as indicated in the figure. An N/C ratio of 0.7, was used for all three cathode layers. The cell was thermostated at 40 °C and 1 M methanol solutions at 2 ml min^{-1} was fed to anode, while the cathode was fed with O_2 at 100 sccm.

fore, for a fair comparison of FC performance, MEA's of optimised, Nafion content, as well as the carbon support, are important.

Figure 8 (a) and (b) show the DMFC performances at 40 and 70 °C, respectively, using KB-60, VC-60 and HG-60 cathode catalysts; however, contrary to Figure 7, optimum N/C ratios are used. At 40 °C and at a cell voltage of 0.4 V, the KB-60 catalyst shows a current density of 128 mA cm^{-2}, which is 1.4 and 2.7 times that of the VC-60 and HG-60 catalyst, respectively. The cathode made using the KB-60 catalyst, in combination with its optimum N/C ratio of 1.4, shows the highest maximum power density of 61 mW cm^{-2}. At 70 °C, Figure 8 (b), the maximum power densities reached for a particular carbon support and their optimum N/C ratio are 109 mW cm^{-2} for KB-60, 92 mW cm^{-2} for VC-60 and 50 mW cm^{-2} for HG-60. The maximal power densities obtained in this work are relative high compared to literature values considering that a total amount of 3 mg cm^{-2} metal catalyst loading and 'not optimised' anodes are used. For example, the maximum power densities for PtRu black and Pt black used as anode and cathode catalysts, respectively with a metal loading of 2 mg cm^{-2} at each electrode (using the same operating conditions as in this work, but, at temperatures of 55 °C) has been reported as 68 mW cm^{-2} [33]. Baglio et al. [34] reported a maximum DMFC power density of 55 mW cm^{-2} at 60 °C using 85 wt% Pt-Ru/C and 60 wt% Pt/C as anode and cathode catalysts, respectively and a Pt loading of 5 mg cm^{-2} for each electrode. The fuel was 1 M methanol at 2 mL min^{-1}, air at 350 sccm and Nafion-117 as membrane. Zhang et al [38]. reported a maximal power density of 46 mW cm^{-2} at 80 °C using a 40 wt% Pt-Ru/C anode catalyst and a 40 wt% Pt/C cathode catalyst and a total metal loading of 2.5 mg cm^{-2} in each electrode. The 2 M methanol

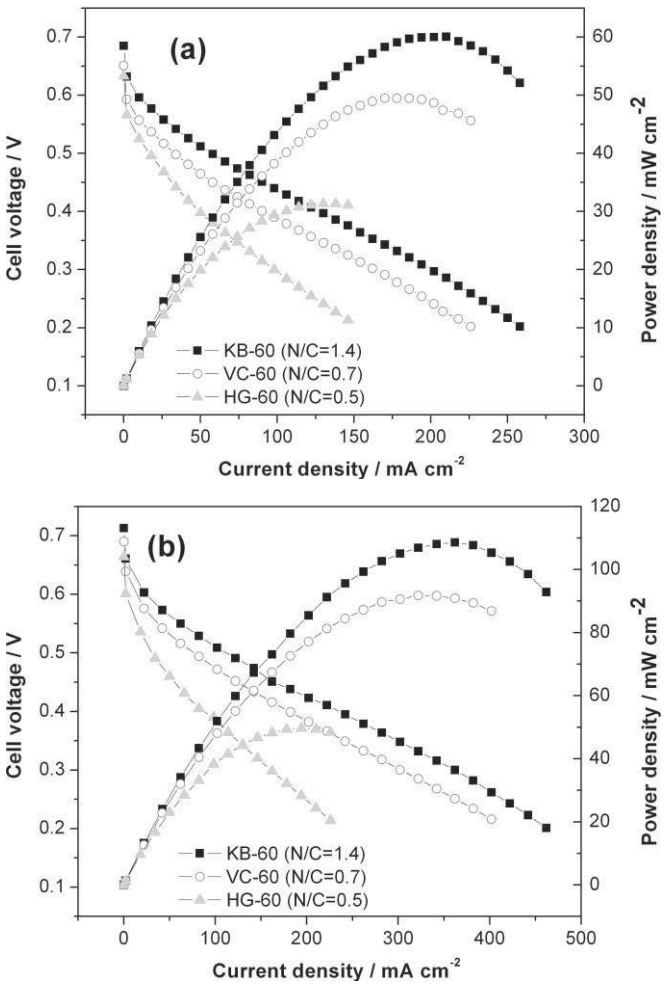

Fig. 8 DMFC performances for KB-60, VC-60 and HG-60 cathode catalysts obtained at (a) 40 and (b) 70 °C. Contrary to the results shown in Figure 7, optimum N/C ratios are used for the three catalysts as follows: 1.4 for KB-60, 0.7 for VC-60 and 0.5 for HG-60.

fuel was supplied at 3 mL min^{-1}, O_2 at 500 sccm, and again Nafion-117 was used as membrane. A very promising DMFC performance was reported by Zhao et al [39]. They reported a maximal power density of 217 mW cm^{-2} at 75 °C for a total Pt + Ru loading of 4 mg cm^{-2}, but, otherwise similar conditions as used in this work [39]. The latter is achieved utilising an optimised anode of 15 wt% Nafion content, i.e. a lower Nafion content than found in this work, which can be explained by the fact that they used unsupported catalysts. It should be noted that comparison of numerical performance values between different laboratories is not entirely valid, as indeed a number of relevant experimental conditions, such as, e.g. the pressure used to compress the cell are typically not reported. Also, the lowering of the total noble metal content without loss of cell performance and durability is a desirable factor for a successful implemanation of DMFCs. A total noble metal loading of 3 mg per cm^2 MEA area appears low compared to results presented over the many past years. However, even this noble metal loading presents a substantial contribution to the total cost of a DMFC.

The results in Figure 8 show that the influence of the carbon support on the DMFC performance is remarkable. KB and VC have the same carbon structure and a similar, as well as large, pore volume (Table 1). However, KB has a smaller average particle size and high surface area. Tada [8] used carbon supports with surface areas varying between 60 and 1300 m^2 g^{-1}. In his case, he found an almost linear increase of catalyst mass activity with the carbon support surface area. The structure of high surface area graphite (HG) is very different from KB and VC. The graphite particles are platelets, rather than spheres, which is the case for the latter two. Although the HG and VC supports have the same surface area, the DMFC using the VC as catalyst support shows a better performance. This difference may be due to differences in the pore-size distribution of the supports. Uchida et al. [9] reported that improvement of DMFC performance can be achieved using a carbon support with a large pore volume, which is able to distribute the Nafion ionomer over the Pt particles inside the carbon support agglomerates.

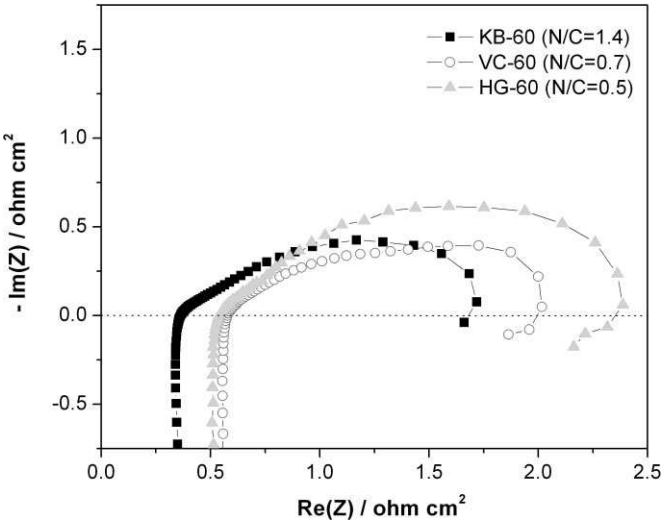

Fig. 9 Electrochemical impedance spectra for KB-60, VC-60 and HG-60 cathode catalysts using optimised N/C ratios as follows: 1.4 for KB-60, 0.7 for VC-60 and 0.5 for HG-60. The total cell impedance shown is obtained in the DMFC working mode at 100 mA cm^{-2} and at a cell temperature of 40 °C.

Figure 9 shows the Nyquist plots for the total cell impedance using KB-60, VC-60 and HG-60 cathode catalysts. The EIS spectra were collected at 40 °C at a current density of 100 mA cm^{-2}. Again, the anode composition, and hence the measured anode impedance, are the same for all of the MEAs. The total cell impedance reflects the resistance of the cathode and the anode. The MEA made of the KB-60 cathode catalyst appears to show the smallest uncompensated as well as charge transfer resistance, although the difference to the cathode layer made using the VC-60 catalyst is not large. The MEAs made using VC and HG cathode catalyst supports have almost the same uncompensated resistance. However, the HG-60 cathode catalyst layer shows a higher ORR charge transfer resistance. The less favoured charge transfer resistance observed for the cathode made using the HG-60 catalyst could be linked to its pore structure, i.e. the lack of a mesoporous structure. The latter is believed to facilitate fuel and reactant transport and to assist with the distribution of Nafion in the catalyst support, and hence, also the utilization of the catalyst sites.

3.3 Effect of Pt Loading in Cathode Catalyst Layer on the DMFC Performance

The effect of the cathode catalyst loading on the DMFC performance was investigated in the range of 0.5 to 2 mg Pt cm^{-2} using the KB-60 catalyst and the optimised N/C ratio of 1.4. Figure 10 (a)–(c) show the DMFC performance curves at 40, 60 and 70 °C, as a function of the Pt loading. For all temperatures, an increase in the Pt loading from 0.5 to 1 mg cm^{-2} results in an increase in the cell voltage at a given current density. The cell voltage is highest for a Pt cathode loading of 1 mg cm^{-2}. Upon increasing the Pt loading from 1 to 2 mg cm^{-2}, the cell voltage decreases significantly. This is believed to be due to mass transport limitations typically caused by thick catalyst layers, while the lower performance observed for the 0.5 mg cm^{-2} Pt cathode loading may be linked to methanol cross-over. The thicknesses of the cathode electrodes (d_c) and MEAs (d_{MEA}) for the different Pt loadings are listed in Table 4. As expected, the thicknesses of the cathode layer and MEAs increase with increasing Pt loading. The calculated differences in d per one mg Pt cm^{-2} loading

Table 4 Electrode parameters for different Pt loadings using the KB-60 cathode catalyst and an N/C ratio of 1.4.

Pt loading[(a)] / mg cm^{-2}	d_c[(b)] / µm	Δd_c/ ΔPt loading[(c)] / µm mg^{-1} cm^2	d_{MEA}[(b)] / µm	Δd_{MEA}/ΔPt loading[(c)] / µm mg^{-1} cm^2	$R_{C\Omega}$[(d)] / Ω cm^2	R_{CCT}[(d)] / Ω cm^2
0.5	230	70	546	22	0.14	0.305
1	264	69	555	20	0.05	0.3
1.5	277	55	564	19	0.1	0.32
2	296	51	569	17	0.12	0.32

[(a)] Pt loading in the cathode per membrane area.
[(b)] Thickness of cathode (d_c) and MEA (d_{MEA}) measured using a micrometer. d_c is measured prior to hot-pressing and includes the carbon paper backing (195 µm). The thickness of MEA is 535 µm measured without the cathode catalyst layer.
[(c)] Changes in d_c and d_{MEA} per mg Pt per cm^2 calculated using the above listed d_c and d_{MEA} measurements and by subtracting 195 µm (carbon paper backing) and 535 µm MEA measured without cathode catalyst layer), respectively.
[(d)] Impedance for the cathode measured as described in Section 3.1.2. $R_{C\Omega}$ and R_{CCT} stand for the uncompensated cathode and the cathode charge transfer resistance towards the orr, respectively. The values shown in Table 4 are extracted from the Nyquist plots shown in Figure 11 (a) and (b).

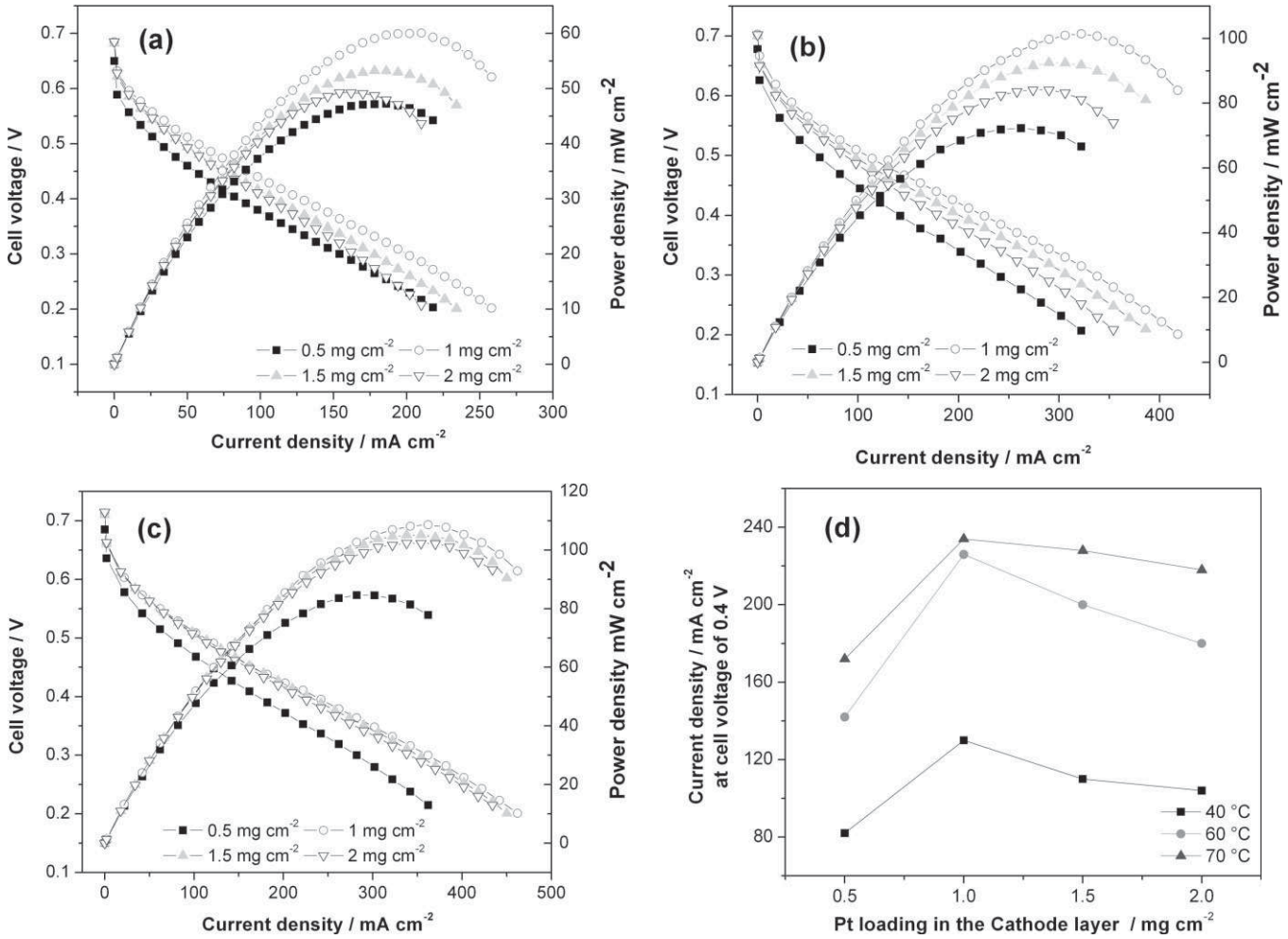

Fig. 10 DMFC performances as a function of the Pt loading in the cathode layer for the example of the KB-60 catalyst and its optimum N/C ratio of 1.4. (a) shows the results for a 40 °C cell temperature, (b) for 60 °C and (c) for 70 °C. (d) shows the relationship between the Pt loading and the current density measured at a cell voltage of 0.4 V. An anode catalyst loading of 2 mg PtRu per cm^2 is used.

($\Delta dc/\Delta Pt$) are also listed in Table 4. The values for the cathode ($\Delta d_c/\Delta Pt$), that are measured prior to hot-pressing, suggest a cathode layer thickness in the range of 50–70 µm per mg Pt cm^{-2}. Hot-pressing decreases the thickness and more reproducible values are obtained, as seen in column 5 in Table 4 where a cathode layer thickness of 17–22 µm per mg Pt cm^{-2} loading is suggested. These numbers are specific for the KB-60 catalyst and the N/C ratio of 1.4. A thickness of 17–22 µm, for a 1 mg Pt cm^{-2} loading cathode catalyst layer, is still high, and in reality thinner electrode layers are desired. Figure 10 (d) shows the current density of the cell at 0.4 V as a function of the Pt loading of the cathode and the different temperatures. The current density is higher at higher temperatures. This behaviour is well known and is due to lowering the activation energy according to the Arrhenius relationship. For a cell temperature of 70 °C, the current and power density is not strongly dependent on the Pt loading for the 1, 1.5 and 2 mg cm^{-2} Pt loading cathodes for unknown reasons.

Figure 11 (a) and (b) show the EIS results of the total and anode impedance for different Pt loadings. The KB-60 cath-

Table 5 Cathode layer parameters for different supports and Pt/C loadings[a].

Support	Wt% Pt/C	d_{Pt}[b] / nm	EASA[c] / $m^2\ g^{-1}$	d_{MEA} / µm
KB	20	1.6	126	682
	40	2	91	581
	60	2.2	78	546
	80	2.5	49	502
VC	20	3	95	585
	40	3.3	67	556
	60	3.5	61	534
	80	4.2	43	528
HG	20	3.3	59	562
	40	3.7	52	552
	60	3.7	50	537

[a] The following N/C ratios are used: 1.4 for KB, 0.7 for VC and 0.5 for HG.
[b] Average Pt crystallite size (d_{Pt}) estimated from XRD patterns using Scherrer's equation and the highest intensity, i.e. the Pt(220) peak.
[c] Pt surface area estimated from CO_{ads} stripping experiments using a CO_{ads} stripping charge to Pt surface area conversion factor of 420 µC cm^{-2}. Measurements were carried out in the FC using 1 mg Pt cm^{-2} loadings in the cathode layer.
[d] Thickness of the cathode measured prior to hot-pressing for 1 mg Pt cm^{-2} loadings. The thickness of the carbon paper backing (195 µm) is subtracted.

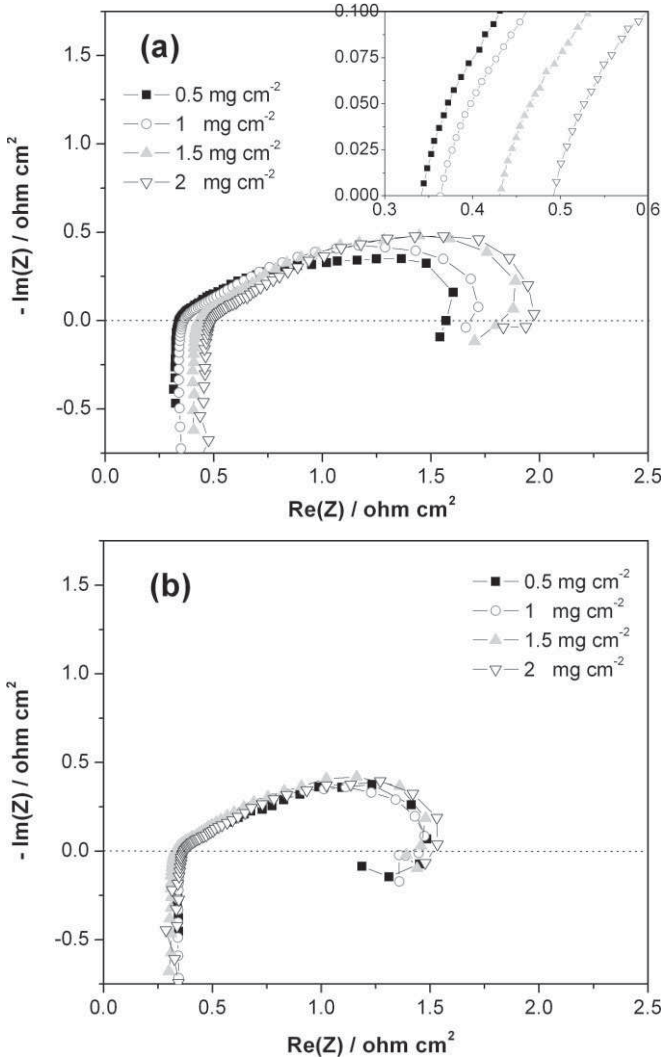

Fig. 11 Electrochemical impedance spectra for different Pt loadings of the cathode. The total cell impedance shown in (a) is obtained in the DMFC working mode at 100 mA cm^{-2}. The cell temperature is 40 °C, 1 M methanol at 2 mL min^{-1} and O_2 at 100 sccm are supplied to the anode and cathode, respectively. (b) shows the anode impedance obtained using the same condition as used for (a), except that the cathode is used as DHE, as described in the experimental section.

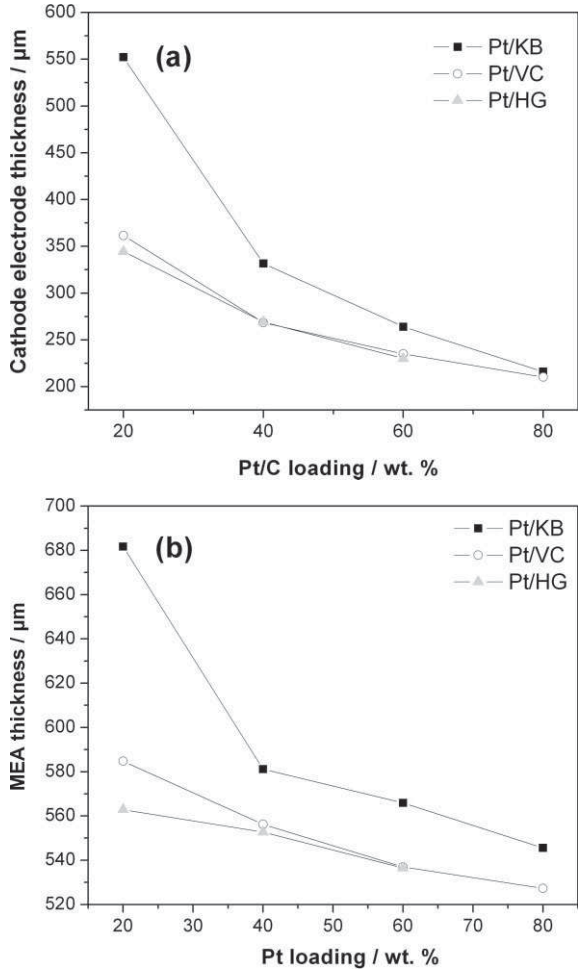

Fig. 12 The relationship between the Pt/C loading of the cathode and the resulting thickness of (a) the cathode electrode and (b) the total MEA . All three supports are tested, as indicated in the figure. The cathode electrode thickness shown in Figure 12 (a) includes the carbon backing paper that measures 195 µm. Two milligram of PtRu cm^{-2} and one milligram of Pt cm^{-2} are used in the anode and cathode catalyst layer, respectively. The following optimum N/C ratios are used: 1.4 for the KB, 0.7 for the VC and 0.5 for the HG support.

ode catalyst was used and the measurements were carried out at 40 °C at a current density of 100 mA cm^{-2}. $R_{\Sigma\Omega}$ and $R_{\Sigma CT}$ increase with increasing Pt loading (Figure 11 (a)). The anode composition is the same for all MEAs, and the anode impedance curves are the same (Figure 11 (b)). Therefore, the increase in the overall resistance directly indicates increase in the $R_{C\Omega}$ and R_{CCT}. The calculated (total cell impedance minus anode impedance) $R_{C\Omega}$ and R_{CCT} values of the cathode catalyst layer are also listed in Table 4. The results indicate that $R_{C\Omega}$ increases with increasing Pt per cm^2 loading, while the R_{CCT} value is suggested to strongly increase from 0.5 to 1 mg Pt cm^{-2}, and a slight increase for the higher (> 1 mg Pt cm^{-2}) Pt per cm^2 loadings.

It should be noted that the long term performance of these catalyst layers needs to be investigated. Initial work in our laboratory has shown that the decay in the DMFC performance of MEAs made using KB-60 as cathode catalyst is relatively small. Over a period of 500 h tested at 100 mA cm^{-2} and at 40 °C, a decay in the DMFC performance of 14% is observed. These are intial results and longer stability studies are currently carried out. Furthermore, additional studies including the influence of higher DMFC opearting tempeartures will also be carried.

3.4 Effect of Reducing the Cathode Layer Thickness (Higher Pt/C Loadings) on the DMFC Performance

The effect of reducing the cathode layer thickness was investigated by comparing the DMFC performance using various Pt/C loadings for all three supports. The Pt loading was 1 mg cm^{-2} at the cathode and the N/C ratios were 1.4, 0.7 and 0.5 for the KB, VC and HG supports, respectively. As for the

previous studies carried out in this work, the anode electrode composition was the same in all cases. Figure 12 (a) and (b) show the relationship between the Pt loading and the cathode electrode thickness and MEA thickness, respectively, for the three carbon supports. As expected in all cases, the cathode and MEA thickness decrease upon increasing the Pt/C loadings. It should be noted that measurements using HG-80 as cathode catalyst were not carried out, as the DMFC performance is not strongly dependent on the wt% Pt/C loading in the case of the HG support (see following paragraphs).

Figure 13 shows the cell performances at 40 °C for the different Pt loadings for all three supports. In the case of the KB support, Figure 13 (a), the 60 wt% Pt/KB catalysts clearly shows the best performance. For example, at 150 mA cm^{-2} the cell potential is 36 and 126 mV higher than for the 40 and 20 wt% Pt/KB cathode catalysts, respectively. The 60 wt% Pt/KB cathode electrode is 264 μm thick (which includes the carbon paper and is measured prior to hot-pressing the entire MEA). The electrodes made using the 40 and 20 wt% Pt/KB catalysts are measured to be 331 and 552 μm thick (Figure 13 (a)), respectively. For such thick cathodes, it is likely that a part of the electrode is inactive due to oxygen and proton diffusion limitations. Nevertheless, the performance for the thinnest cathode made using the 80 wt% Pt/KB catalyst is lower than for the cathode made using the 60 wt% Pt/KB catalyst. This behaviour could be due to a decrease in the electroactive Pt surface area from 78.3 to 48.6 m^2 g^{-1} for the 60 and 80 wt% Pt/KB catalysts. A higher DMFC performance may be achieved using a smaller Pt particle size in combination with the higher loading (>80 wt% of Pt on the C support).

In the case of the VC support, Figure 13 (b), the trends are similar to the results obtained using the KB support, while the DMFC performance is not strongly dependent on the wt% Pt/C in the case of the HG catalyst support, Figure 13 (c).

As shown in Table 5, for the KB support, XRD results suggest that the average Pt crystallite size of the 'as prepared' catalyst increases from 1.6 to 2.5 nm with increasing the Pt loading from 20 to 80 wt%. For the VC support, the average Pt crystallite size increases from 3 to 4.2 nm, and similar changes are observed for the HG support. An increase in Pt particle size results in a lower Pt surface area per weight of catalyst. However, the higher loading Pt/C catalysts may be closer to the optimal Pt particle size for the ORR, the influence of which has not been studied in this work.

4 Conclusion

A range of home-made Pt catalysts on different supports are studied in this work for their potential application in cathode catalyst layers in DMFCs. The optimal Nafion of the cathode catalyst layer is determined, which was found to depend on the support, rather than the Pt/C loading. This is believed to be linked to different properties of the support, such as particle size and micro-porosity. The Pt catalysts were made using a particular colloidal synthesis route. Despite the fact that the same colloidal catalyst solution was used, the average Pt particle size and EASA is found to depend on Pt/C loading as well as on the support in this work. For the catalysts prepared in this work, the average Pt particle size (determined by XRD) decreases with an increase in the surface area of the support for a particular Pt/C loading. DMFCs made using KB as cathode catalyst support, in combination with the optimised Nafion content, show better performance in comparison with the VC and HG supports. For all the cathode catalysts studied, the highest DMFC performance was found for a 60 wt% Pt/C loading on KB using the Nafion to carbon plus catalyst (N/C) ratio of 1.4. KB is the support with the highest surface area, ~1300 m^2 g^{-1} *versus* 250 m^2 g^{-1} for VC and HG. The dispersion of the Pt catalyst and the active catalyst surface area are also the highest for the cathode made using this catalyst and Nafion content, thus likely accounting for the higher performance. Consistent with the highest performance, the resistance of the cathode is also the smallest for this cathode. This further confirms the improved performance. For a particular Pt/C loading, the Pt particle size was found to be the smallest using the KB support. It should be noted that this results applies to the catalyst preparation procedure used in this work and may be indeed be found to be different in other studies. The particle size is, however, smaller (namely 2 nm for 60 wt% Pt on KB) than the generally proposed optimal Pt particle size of ~3.5–4 nm for the ORR. It has not been clarified in this work if the smaller Pt particle size is beneficial or detrimental to the DMFC performance. It should also be noted that the Pt particle sizes listed in this work are average size determined from XRD patterns and determined for as prepared catalysts.

The DMFC performance was also tested for different Pt per cm^2 loadings, namely 0.5 to 2 mg Pt cm^{-2}. A maximal DMFC performance was observed for cathodes made using 1 mg Pt cm^{-2}. It is possible that the lower performance for the thinner Pt cathode (0.5 mg Pt cm^{-2}) is due to methanol crossover, while the lower performance for the higher loadings (1.5 and 2 mg Pt cm^{-2}) may be due to mass-transport limitations of O_2 fuel and limited proton conductivity within the thicker catalyst layers. The use of the high Pt/C loading, i.e. the 60 wt% Pt/C cathode catalysts, increases the effective catalyst surface area in the active region of the cathode. This results in increased DMFC performance compared to electrodes with 20 and 40 wt% Pt loading catalysts. A further increase in the Pt/C loading of the catalyst to 80 wt% Pt/C was found not to be beneficial, even though the cathode electrode thickness was lower.

Acknowledgment

We thank TIMCAL Graphite & Carbon for providing the HSAG graphite sample. Financial support from NRC-NSC-ITRI (Canada/Taiwan) fund and DND are also gratefully appreciated.

References

[1] E. Reddington, A. Sapienza, B. Gurau, R. Viseanathan, S. Sarangapani, E. S. Smotkin, T. E. Mallout, *Science* **1998**, *280*, 1735.
[2] A. Hamnett, *Catal. Today* **1997**, *38*, 445.
[3] M. P. Hogarth, G. A. Hards, *Platinum Metal Reviews* **1996**, *40*, 150.
[4] H. F. Oetjen, V. M. Schmidt, U. Stimming, F. Trila, *J. Electrochem. Soc.* **1996**, *143*, 3838.
[5] K. W. Park, J. H. Choi, B. K. Kwon, S. A. Lee, Y. E. Sung, H. Y. Ha, S. A. Hong, H. Kim, A. Wieckowski, *J. Phys. Chem. B* **2002**, *106*, 1869.
[6] T. Navessin, M. Eikerling, Q. Wang, D. Song, Z. Liu, J. Horsfall, K.V. Lovell, S. Holdcroft, *J. Electrochem. Soc.* **2005**, *152*, A796.
[7] J. Zhang, Z. Xie, Y. Tang, C. Song, T. Navessin, K. Shi, D. Song, H. Wang, D. P. Wilkinson, Z. Liu, S. Holdcroft, *J. Power Sources* **2006**, *160*, 872.
[8] T. Tada in *Handbook of Fuel Cells*, *Vol. 3* (Eds. W. Vielstich, A. Lamm, H. Gasteiger), WILEY-VCH, New York, **2003**, pp. 481.
[9] M. Uchida, Y. Fukuoka, Y. Sugawara, N. Eda, A. Ohta, *J. Electrochem. Soc.* **1996**, *143*, 2245.
[10] M. Uchida, Y. Anoyama, N. Eda, A. Ohta, *J. Electrochem. Soc.* **1995**, *142*, 4143.
[11] E. Antolini, L. Giorgi, A. Pozio, E. Passalacqua, *J. Power Sources* **1999**, *77*, 136.
[12] S. C. Thomas, X. Ren, S. Gottesfeld, *J. Electrochem. Soc.* **1999**, *146*, 4354.
[13] G. Sasikumar, J. W. Ihm, H. Ryu, *J. Power Sources* **2004**, *132*, 11.
[14] T. V. Reshetenko, H.-T. Kim, H. Leem, M. Jang, H.-J. Kweon, *J. Power Sources* **2006**, *160*, 925.
[15] A. J. Appleby, E. B. Yeager, *Energy* **1986**, *11* 137.
[16] E. Passalacqua, F. Lufrano, G. Squadrito, A. Patti, L. Giorgi, *Electrochim. Acta* **2001**, *46*, 799.
[17] S. Gamburzev, A. Appleby, *J. Power Sources*, **2002**, *107*, 5.
[18] Z. Qi, A. Kaufman, *J. Power Sources* **2003**, *113*, 37.
[19] F. Liu, C-Y. Wang, *Electrochim. Acta* **2006**, *52*, 1409.
[20] J. M. Song, S. Suzuki, H. Uchida, M. Watanabe, *Langmuir* **2006**, *22*, 6422.
[21] M. S. Wilson, S. Gottesfeld, *J. Appl. Electrochem.* **1992**, *22*, 1.
[22] C. Bock, C. Paquet, M. Couillard, G. A. Botton, B. R. MacDougall, *J. Am. Chem. Soc.* **2004**, *126*, 8028.
[23] E. A. Baranova, C. Bock, D. Ilin, D. Wang, B. MacDougall, *Surf. Sci.* **2006**, *600*, 3502.
[24] Y. Takasu, T. Fujiwara, Y. Murakami, K. Sasaki, M. Oguri, T. Asaki, W. Sugimoto, *J. Electrochem. Soc.* **2000**, *147*, 4421.
[25] T. Kawaguchi, W. Sugimoto, Y. Murakami, Y. Takasu, *Electrochem. Commun.* **2004**, *6*, 480.
[26] J. T. Müller, P. M. Urban, W. F. Hölderich, *J. Power Sources* **1999**, *84*, 157.
[27] J. T. Müller, P. M. Urban, *J. Power Sources* **1998**, *75, 139.*
[28] T. V. Reshetenko, H.-T. Kim, H. Lee, U. Krewer, H.-J. Kweon, *Fuel Cells* **2007**, *3*, 238.
[29] A. Pozio, M. De Francesco, A. Cemmi, F. Cardellini, L. Giorgi, *J. Power Sources* **2002**, *105*, 13.
[30] A. V. Radmilovic, H. Gasteiger, P. Ross, *J. Catal.* **1995**, *154*, 98.
[31] A. Havránek, K. Wippermann, *J. Electroanal. Chem.* **2004**, *567*, 305.
[32] L. Birry, C. Bock, X. Xue, R. McMillan, B. MacDougall, *J. Appl. Electrochem.* **2008**, *39*, 347.
[33] M. K. Jeon, J. Y. Won, K. S. Oh, K. R. Lee, S. I. Woo, *Electrochim. Acta* **2007**, *53*, 447.
[34] V. Baglio, A. Stassi, A. Di Blasi, C. D'Urso, V. Antonucci, A. S. Aric$ograve$, *Electrochim. Acta* **2007**, *53*, 1360.
[35] K. Kinoshita, *J. Electrochem. Soc.* **1990**, *137*, 845.
[36] F. Maillard, M. Martin, F. Gloaguen, J.- M Léger, *Electrochim. Acta* **2002**, *47*, 3431.
[37] W. Li, C. Liang, W. Zhou, J. Qiu, H Li, G. Sun, Q. Xin, *Carbon* **2004**, *42*, 423.
[38] J. Zhang, G.-P. Yin, Z.-B. Wang, Q.-Z. Lai, K.-D. Cai, *J. Power Sources* **2007**, *165*, 73.
[39] X. Zhao, X. Fan. S. Wang, S. Yang, B. Yi, Q. Xin, G. Sun, Internat. *J. Hydrogen Energy* **2005**, *30*, 1003.

